Proceedings World Geothermal Congress 2023
Beijing, China, April 17 – 21, 2023

Performance Analysis of Oval and Circular Cross-Sections Single U-Tube Ground Heat Exchangers: A Simulation-Based Comparison

Taha Rajeh[1, 2], Basher Hassan Al-Kbodi[1], Yang Li[1, *], Jun Zhao[1, *]

[1]Key Laboratory of Efficient Utilization of Low and Medium Grade Energy (Tianjin University), Ministry of Education of China, Tianjin 300350, China

[2] Faculty of Engineering, Thamar University, Dhamar PO Box 87246, Yemen

[*] Corresponding author: zhaojun@tju.edu.cn (J. Zhao), liyangtju@tju.edu.cn (Y. Li).

Keywords: Ground-coupled heat pump; ground heat exchanger; thermal performance; numerical simulation; single U-tube

ABSTRACT

The heat transfer performance of vertical Ground Heat Exchangers (GHEs) is an important criterion for this key component of Ground Source Heat Pump (GSHP) systems. This paper examines the thermal efficiency of oval cross-section single U-tube GHE compared to circular cross-section single U-tube GHE to evaluate the geometrical configurations and physical properties of the oval cross-section single U-tube GHE. The impact of key operating and design parameters on the thermal performance of the GHEs is also investigated, followed by a detailed sensitivity analysis. The analysis is performed by means of a three-dimensional numerical model. Experimental data from the literature are used to validate the adopted numerical model. The results showed that the maximum and average heat transfer rate of the oval cross-section GHE could be increased by 26.41% and 12.26% compared with circular cross-section GHE. The results of the sensitivity analysis revealed that flow rate, GHE material's thermal conductivity, GHE length, and tube cross-section area have the highest impact on the thermal performance of the oval cross-section GHE. Therefore, these parameters should be carefully designed. However, the effects of these parameters are dominant early in the heat exchange operation. The outcomes of this study can substantially give guidance for the favorable configuration from the heat transfer performance perspective.

1. INTRODUCTION

Geothermal energy, as a sustainable and plentiful energy source, has the potential to replace fossil fuels and thus promote environmental protection and global energy security. Studies have demonstrated that the GSHP system occupies a 59.20% of the geothermal energy utilization annually and is widely recognized as a highly influential and promising method for geothermal energy conversion (Dores and Lautze, 2020; Lund and Toth, 2021). The influence of ground thermal inertia on the soil surface temperature causes the ground temperature to be higher than the ambient air temperature during the winter and lower during the summer. Consequently, the GSHP system is significantly more efficient than an ASHP system (Dores and Lautze, 2020).

The GSHP system generally comprises a ground heat exchanger (GHE), a heat pump, and a distribution system (Self, Reddy and Rosen, 2013). GHE, as a main component of the GSHP systems, is classified into two general types: horizontal GHEs and vertical GHEs, according to the installation depth. The vertical GHE, normally built within a depth of up to 200 m, is more commonly used than the horizontal GHEs due to its smaller land occupation and improved heat transfer efficiency (Yang, Cui and Fang, 2010). However, its main drawback is its drilling and installation costly expenses. Besides, the GHE comes directly in contact with the heat source/sink (i.e., the GHE surroundings), compromising the GSHP system's effectiveness. Consequently, GHEs are the most significant constituent of the GSHP system and must be precisely designed.

One of the most critical components of the GHE is the pipe layout type and pipe cross-section shape (i.e., pipe configuration) (Noorollahi et al., 2018; Ngo and Ngo, 2022), which recently attracted the majority of scientists and manufacturers in this field. The alternatives of the pipe layout types such as the conventional single U-tube (Kerme and Fung, 2020), double U-tube (2U) (Kerme and Fung, 2021a), multiple-tubes (Song et al., 2017), W type (Mehrizi et al., 2016) and multiple W type (Song et al., 2017), helical (Zarrella, Capozza and De Carli, 2013), or a combination of alternatives of these types (Javadi, Mousavi Ajarostaghi, et al., 2019) were being adopted aiming to augment the heat exchange efficiency of the GHE with the various influences. However, helical GHE and multi-tube GHE typically require a larger borehole diameter, 2-4 times the standard diameter (Zarrella, De Carli and Galgaro, 2013; Aydın and Sisman, 2015). Furthermore, a support structure is needed to support its shape, making the GHE production and installation more challenging and expensive (Zarrella, De Carli and Galgaro, 2013; Aydın and Sisman, 2015; Saeidi, Noorollahi and Esfahanian, 2018). As a result, helical GHE and multi-tube BHE are more proper for energy pile applications (Zhao, Li and Wang, 2016).

All the studies mentioned above on GHE pipeline are classified under the circular cross-section shape GHE types. However, changing the shape of the pipe cross-section could influence its thermal performance more economically and reliably than modifying its structure (e.g., pipe cross-section shape, heat conducting fin). Therefore, recent studies have also investigated novel cross-section shapes of the GHE tubes to increase the GHE thermal efficiency and reduce the borehole depth, decreasing its drilling and set-up expenses. (Jahanbin, 2020) proposed a novel elliptical U-tube cross-section. Their results demonstrated that elliptical U-tube could improve heat exchange and reduce thermal resistance by over 17% compared to standard circular shape U-tubes. (Serageldin et al., 2018; Serageldin, Radwan, et al., 2020; Serageldin, Sakata, et al., 2020) performed several studies on a novel oval U-tube cross-section GHE with and without a spacer, besides studying the underground flow effect. Their results showed that the oval shape has a better heat transfer performance with the minimum borehole thermal resistance of 0.125 m.K/W, in which the thermal resistance decreases by 18.47% compared to the circular shape using a spacer could considerably improve the heat transfer effectiveness. (Zhou et al., 2021) studied the thermal performance of the GHE with various shapes of U-tube GHEs (flat oval, curved oval, semicircle, sector, and circle). Their results revealed that changing the shape of the U-tube could enhance the thermal performance of GHEs, and they concluded that the U-tube with a flat oval shape was the best U-tube-shaped design for GHEs.

Studies on the cross-sectional shape of GHEs are limited. Based on the studies mentioned above, oval cross-section pipe U-tube GHE is a promising GHE design that could contribute to the design and development of GSHPs. However, a detailed of the critical design and operating parameters using the heat flux as a heat transfer evaluation parameter and a comprehensive sensitivity analysis of oval cross-section pipe U-tube GHE compared to conventional circular cross-section pipe U-tube GHE have not been introduced before.

This study investigates the thermal performance of the oval cross-section U-tube GHE compared to the circular cross-section U-tube GHE by providing a systematic comparison with a total of 10 key operating and design parameters. In addition, a comprehensive sensitivity analysis is conducted. More perspective into the differences in heat exchange performance can be gained by systematically conducting simulations that consider the proposed U-tube designs under comparable conditions; this is achieved by simulating the proposed designs with equal pipe cross-sectional area and consistent inlet flow conditions and thermophysical properties. It is essential that the modeling used to compare the GHE effectiveness catches the heat transfer behavior at all timeframes. Therefore, for this study, a three-dimensional, unsteady state numerical model validated by experimental data from the literature was selected. This model accurately captures the proposed GHE's short and long-term behavior, allowing a comprehensive analysis of the changes in heat transfer performance throughout the GHEs.

2. MODELS

4.1 Geometric model

Figure 1 illustrates the cross sections of the studied tube-shaped. The geometry models in this paper consist of four domains: a heat carrier fluid domain (i.e., water in this paper) circulating inside a single U-tube with a circular or oval tube domain inside a borehole surrounded by the backfill material (i.e., which is the same as the soil in this paper), then the soil domain. Table 1 illustrates the parameters description section of the circular and oval tubes GHEs. Since the down part of the heat exchanger, where flow reverses, is small in comparison to the entire length of the GHEs, this portion of the heat exchangers and the ground beneath the GHEs were overlooked. Accordingly, the geometric models do not take into account this part. A user-defined function (UDF) was used to connect the tube bottoms so that the temperature of the bottom part of the flow entering the tube is equal to the entrance temperature of the flow leaving the GHE tube.

To better compare the effect of the tube cross-section shape on the thermal performance of the proposed GHEs and to guarantee a justified comparison study, the geometrical parameters of the oval tube (width (w), and height (*h*), see Figure 1 and Table 1) were adjusted to ensure that the cross-sectional area of the oval tube is consistent with the circular tube as 835 mm^2 (Serageldin et al., 2018; Zhou et al., 2021).

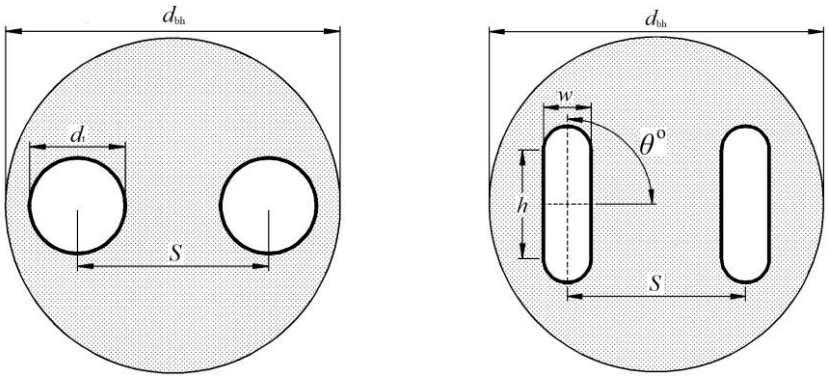

(a) (b)

Figure 1. Cross sections of the studied tube-shaped GHEs: (a) Circular shape, (b) Oval shape.

Table 1. Parameters description of the cross-section.

Tube shape	Parameter	Value	Parameter	Value
Circular	Tube inner diameter (d_t)	32.6 mm	Tube thickness	3.7 mm
Oval	Width (w)	14 mm		
	Height (h)	48.63 mm		
	Inclined angle (θ)	90^o		
Borehole	Diameter (d_{bh})	150 mm	Shank spacing (S)	80 mm
	Depth	120 m	Diameter	8 m

4.2 Three-dimensional numerical model

A widely used in GHE numerical studies, ANSYS FLUENT software (Serageldin et al., 2018; Javadi, Ajarostaghi, et al., 2019; Salmani and Noee, 2022), was selected to build a three-dimensional, unsteady-state numerical model. The SIMPLE scheme was adopted for the pressure-velocity coupling. Second-order upwind was adopted for both energy and momentum in spatial discretization. Furthermore, solution convergence was achieved for each time step of all the simulations in the current study.

2.2.1 Assumptions

The numerical model assumptions are as follows:

1. The thermophysical properties of the soil, water, and tubes are constant, and the fluid flow is incompressible.

2. The undistributed soil temperature is the same as the initial temperature, and the temperature distribution is equal to the initial temperature for the radial boundary of the soil.
3. The impact of groundwater flow is ignored.
4. The heat exchange from the soil surface to the air is overlooked.

2.2.2 Initial conditions and boundary conditions

The initial temperatures of the soil for the GHE simulations at cooling mode were extracted from measured data by the Institute of Tianjin Geothermal Exploration and Development-Designing, and it is available in our previous work (Li et al., 2020). The inlet temperature is constant at 30 ℃, and it satisfies the conditions of the Chinese national standard of ground source heat pump (GB50366-2009) (Ministry of Construction in the People's Republic of China, 2009). The simulation time was selected to be 24 hours. Boundary conditions and physical properties of the GHE materials are shown in Table 2 and Table 3, respectively.

Table 2. Boundary conditions.

GHE structure		Boundary condition
Fluid	inlet	30 ℃, = 0.6 kg/s
	Outlet	P = 0 Pa (gauge)
Solid	Top Surface	Adiabatic
	Bottom surface	Adiabatic
	Outer soil Wall	Constant vertical temperature distribution

Table 3. Material's physical properties.

Part	ρ (kg/m^3)	C_p (J/(kg·K))	λ (W/(m·K))	μ (Pa.s)
Soil	1220	2070	1.50	-
Water	1000	4180	0.60	0.001
GHE (HDPE)	1000	1824	0.4	-

2.2.3 Mesh topology

A grid independence test was performed on the two proposed GHEs to ensure that the meshes were sufficiently refined. The simulation conditions for the mesh tests are shown in Table 2 and Table 3.The outlet temperature (T_o) was monitored during the test while the mesh was adjusted. The relative absolute error of the outlet temperatures of the tests is a negligible error, as shown in Table 4, disclosing that the meshes of the two models were sufficiently refined. The meshes were all structured, with an EquiSize Skew of less than 0.5 in 99.95 % of the meshes in all the simulation cases, including the changing in the geometrical parameters cases. Mesh quality was tested before every simulation case, and its quality was ensured. Since the geometrical shapes of the two proposed GHEs are symmetrical around the horizontal axis, the geometries of the proposed models were divided into two halves of subdomains, and only a half size with asymmetric boundary conditions was analyzed to decrease the computational time, as shown in Figure 2. The ideal mesh element number for the circular and oval tube GHE models are 619080 and 514200, respectively.

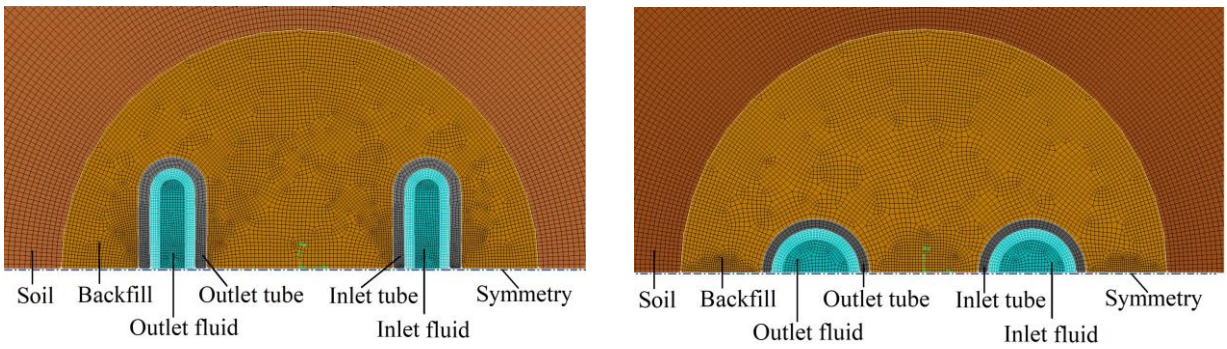

Figure 2. Horizontal grid of the 3-D numerical models. (a) Oval cross-section tube GHE, (b) Circular cross-section tube GHE.

Table 4. Mesh independence check results of the two proposed cross-sectional tube GHE 3-D models.

Circular		Oval	
Number of elements	Average absolute error of T_o (℃)	Number of elements	Average absolute error of T_o (℃)
2476320	0	2056800	0
1238160	0.0001	1028400	0.0002
619080	0.0004	514200	0.0003
309540	0.0007	257100	0.0012
154770	0.0016	128550	0.0037

3. VALIDATION OF THE NUMERICAL MODEL

To validate the adopted numerical studies in this paper, a comparison of the temperature of the outlet water of a single U-tube with circular cross-section GHE based on operation time was made between the simulation results of the adopted numerical model in the current study and the experimental test results of (Jalaluddin et al., 2011). As shown in Figure 3, the adopted numerical model in this paper has excellent accuracy with a mean absolute error of 0.19 ℃ to the experimental data of (Jalaluddin et al., 2011), which validates the accuracy of this paper's numerical studies.

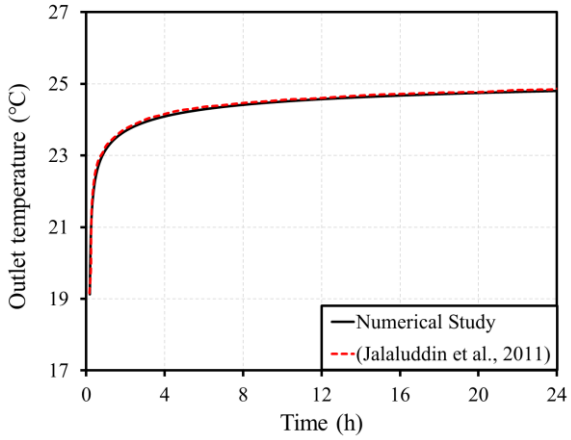

Figure 3. Validation of the numerical model to (Jalaluddin et al., 2011).

4. RESULTS AND DISCUSSIONS

A systematic evaluation comparison was performed on the effect of a number of key design and operating parameters on the thermal performance of the adopted circular and oval tube-shaped GHEs. The following key operating and design parameters were studied: mass flow rate (M), the thermal conductivity of GHE materials (λ_{GHE}), GHE length (L), tube cross-section area (A), thermal conductivity of backfill materials λ_{bf}, soil thermal conductivity λ_s, shank spacing (S), tube thickness (t), shape factor (β), and tube inclined angle (θ^o). In all the cases of the parameters impact evaluation for the two adopted tube-shaped GHEs, the influence of the studied parameters was compared to that of the standard case with the listed geometrical parameters in Table 1, boundary conditions in Table 2, and material's physical properties in Table 3, and then compared the two tube-shaped GHEs to each other. The heat transfer rate per unit length (i.e., heat flux (W/m)) was used as an evaluation parameter.

4.1 The influence of the flow rate

The heat flux per unit length (q) was calculated for the oval and the circle tubes at a given range of mass flow rate (M), and the results are sown in Figure 4. The increase ratio of q_{oval} over $q_{circular}$ (will be represented as Δ in this study) among the selected range of M along the operation time is shown in Figure 4(a). It can be seen that q_{oval} overlaps $q_{circular}$ along the given range of M, and Δ is significantly higher with the higher values of M; this is because the area of the tube surface of the oval tube is larger than that of the circular tube, which means that the heat exchange rate between the fluid inside the tube and the surroundings of the oval tube will be higher compared to the circular tube. Furthermore, this enhancement is significantly high early in the operation, but it decreases gradually to be almost stable at the later stages; this is due to that the surrounding soil and the backfill material are not highly affected by the heat at the early stages of the cooling process. Due to the gradual transfer of heat from the water to the backfill material and soil, q decreases dramatically, and then after six hours, it is stabilized in all cases. To further illustrate the effect of the early stages of the operation, Figure 4(b) shows the average q_{oval} and $q_{circular}$ at 01:00 for the given range of M, and the corresponding Δ. Figure 4(c) shows the water temperature versus the depth of GHE for the proposed tube shapes. According to this figure, the water temperature decreases more within the oval tube than in the circular tube.

These results indicate that the heat exchange performance of oval tube GHE is better than that of the circular tube GHE, particularly at the initial stages of the operation, in which this feature is beneficial for applications that require rapid cooling responses. Furthermore, the enhancement of oval tube GHE over the circular tube GHE could increase with increasing the heat carrier flow rate.

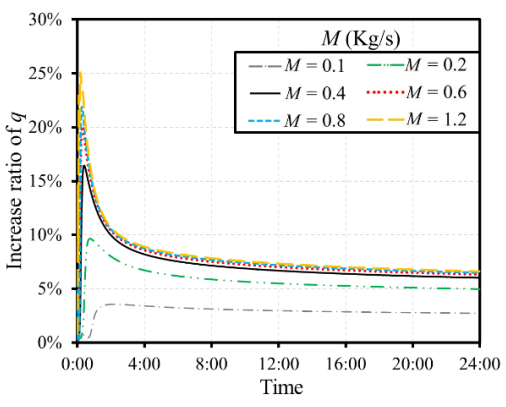

(a)

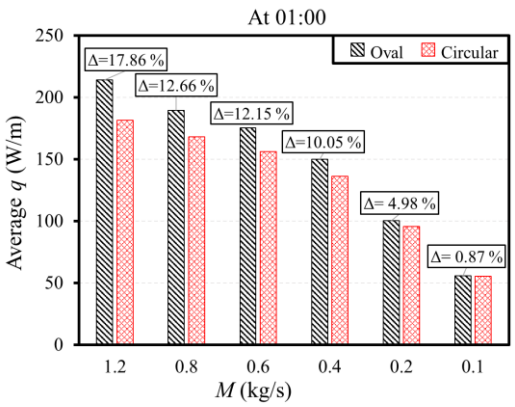

(b)

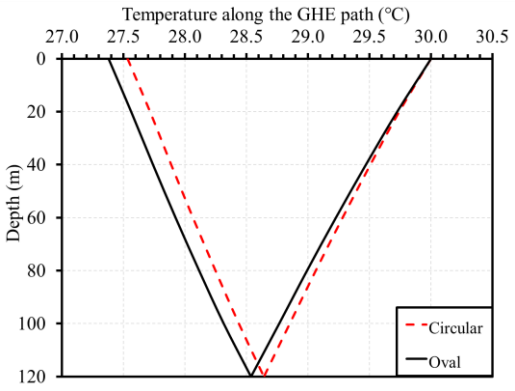

(c)

Figure 4. Comparison results of oval and circular tube GHEs under different flow rates: (a) The increase ratio of q_{oval} over $q_{circular}$ (Δ) at various M (kg/s), (b) Average q at 01:00, and (c) Heat carrier fluid temperature versus depth of oval and circular tube GHEs.

4.2 Thermal conductivity of the GHE materials

Three GHE material's thermal conductivity (λ_{GHE}) (W/m·K) were studied: 0.13, 16.2, and 386, besides the standard case of 0.4 W/m·K, which corresponded to the thermal conductivities of PVC, Aisi304 stainless steel, copper, and HDPE. The change in volumetric heat capacity was not taken into account. Figure 5 shows the comparison results of oval and circular tubes under different λ_{GHE}. At all the given values of λ_{GHE}, q_{oval} is higher than $q_{circular}$, and Δ is the highest with the lower values of λ_{GHE}; this is because decreasing λ_{GHE} will decrease the thermal short circuit effect between the tube legs to a minimum, as reported in previous work (Serageldin, Sakata, et al., 2020). For instance, when λ_{GHE} = 0.13 W/m·K, Δ reaches 26.41 %, and Δ at 24:00 is 12.26 %. Furthermore, the average q of the two proposed tube shapes is increasing with increasing λ_{GHE}, but this increase will have a minimal effect on q at the very high values of λ_{GHE}, particularly in the initial stages of the operation; this is because of the thermal resistance of the surroundings (the soil in this paper) (Tang and Nowamooz, 2019).

As a result, oval tube GHE has a better heat transfer performance than circular tube GHE at the given values of λ_{GHE}, and with lower λ_{GHE}, oval tube GHE transfers more heat than circular tube GHE.

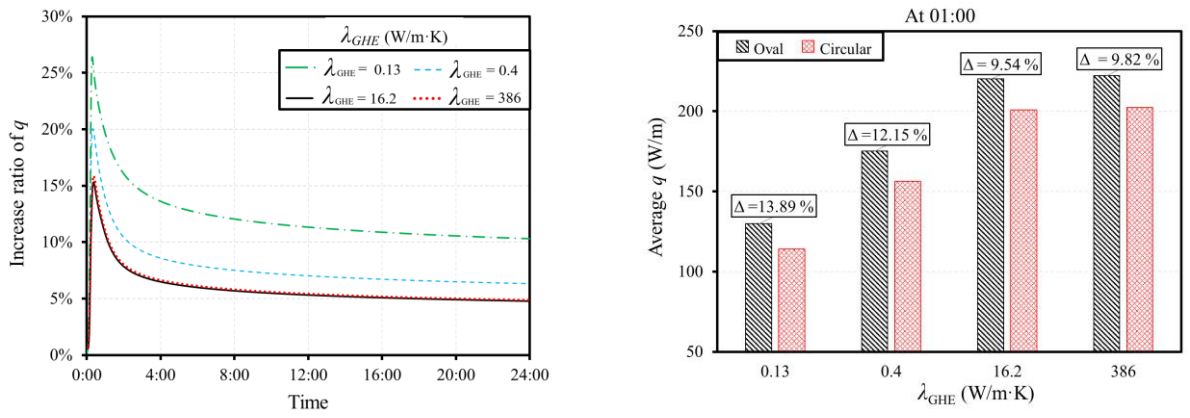

(a) (b)

Figure 5. Comparison results of oval and circular tube GHEs under different λ_{GHE}: (a) Increase ratio of q when M = 0.6 kg/s, (b) Average q at 01:00.

4.3 GHE length

According to the guidebook of ASHRAE (Kavanaugh and Rafferty, 2014), three typical GHE lengths L (m) were selected: 60, 90, and 150; besides, the standard length in this paper 120. The change ratio of average q_{oval} and $q_{circular}$ at different GHE depths along the selected periods is presented in Table 5. The results show that q_{oval} and $q_{circular}$ decrease as L increases; this is because a higher depth of GHE will worsen the thermal short-circuit effect between the tube legs, which will affect the overall GHE performance, as revealed in a previous study (Li et al., 2014; Jahanbin, 2020). A Comparison of oval and circle tubes is shown in Figure 6. Under all the given values of L and along the operation time, q_{oval} is higher than $q_{circular}$, and Δ is increasing by decreasing L. Consequently, the results confirm that oval tube GHEs are more promising for shallower depths than deeper ones.

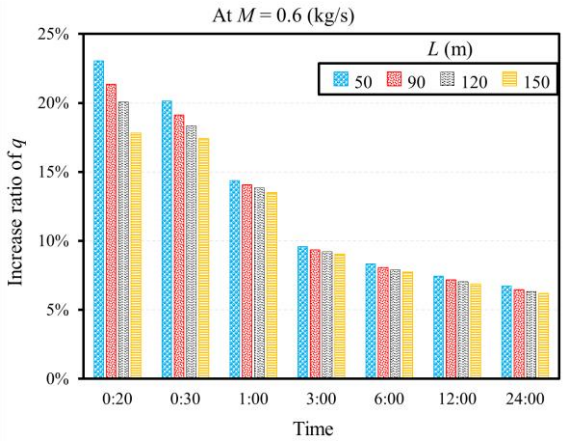

Figure 6. Average q of oval and circular tube GHEs under different L.

4.4 Tube cross-section area

Increasing the heat exchange area of the GHE by increasing the tube diameter leads to an enhancement in the thermal performance of the GHEs (Serageldin et al., 2021). Two more tube cross-section areas A (mm^2) were selected: 530, and 1256, besides the standard value in this paper 385. To guarantee a realistic comparison, the tube thickness for the circle and oval tubs and the shape factor (β) (see Section 4.9) of the oval tube are consistent while studying the effect of A. Table 5 shows the change ratio of average q_{oval} and $q_{circular}$ at different A throughout the operation durations. For the two studied tube-shaped, increasing A will increase q. However, Δ at 01:00, 06:00, and 24:00 is around 13.00%, 10.71%, and 8.32%, respectively, and this increasing percentage is nearly the same in all the studied A values. Consequently, increasing the tube cross-section area will improve the heat transfer performance of the studied tube-shaped. This enhancement is higher for the oval tube than the circular tube GHE, which is consistent with the previous studys' findings (Serageldin et al., 2018).

4.5 Thermal conductivity of backfill materials

Four values of the thermal conductivity of the backfill materials λ_{bf} (W/m·K) were studied: 0.9, 1.2, 2, and 2.5, besides the standard value in this study 1.5. The volumetric heat capacity variation was overlooked. The change ratio of average q_{oval} and $q_{circular}$ with given values of λ_{bf} at various durations is illustrated in Table 5. Generally, for the two proposed tube shapes, as λ_{bf} decreases, q decreases; this is because decreasing q will increase the thermal resistance of the surroundings leading to a deterioration of the heat exchange rate of the GHE. Figure 7 shows average q_{oval} and $q_{circular}$ under different λ_{bf} at 24:00. From Table 5 and Figure 7, q_{oval} is higher than $q_{circular}$; this is because the oval-shaped tube has a larger outer tube surface in contact with the surroundings than the circular-shaped tube, making it more sensitive to the effect of λ_{bf} than the circular tube.

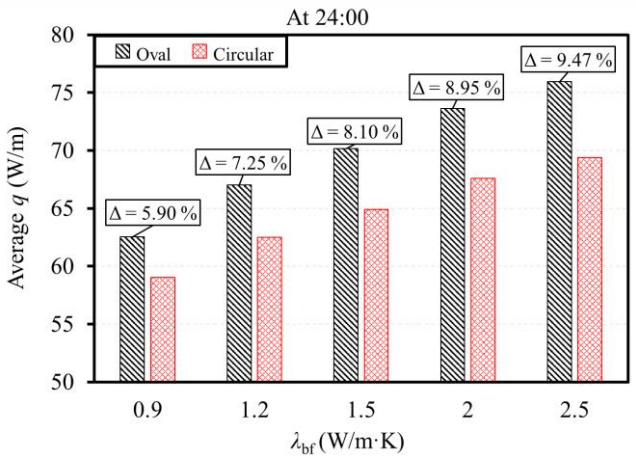

Figure 7. Average q of oval and circular cross-section tube GHEs under different λ_{bf} at 24:00.

4.6 Thermal conductivity of soil

Three typical soil thermal conductivity λ_s (W/m·K) from Tianjin city (Ruan C, Feng S, 2017) were selected: 1.27, 1.34, and 1.62, besides the standard value in this paper 1.5. The volumetric heat capacity variation was overlooked. Table 5 depicts the change ratio of average q_{oval} and $q_{circular}$ along the various operation durations under the given values of λ_s. Generally, the average q of oval and circular tubes increases with increasing λ_s. However, early in the operation, the influence of λ_s on the two proposed tube shapes is modest; while the time of the operation increases, the effect of λ_s rises. However, with all the selected λ_s values, q_{oval} outperforms $q_{circular}$.

4.7 Shank spacing

Based on the maximum and minimum shank spacing of the circular tube, since the radius of the inner circular tube is larger than the width parameter of the oval tube shape (see Table 1), the studied shank spacing S (mm) values were selected as 40, 60, and 110, besides the standard value in this study 80. The change ratio of average q_{oval} and $q_{circular}$ throughout various operation durations under the given values of S is shown in Table 5. Generally, decreasing S will reduce q_{oval} and $q_{circular}$; because decreasing the shank spacing will worsen the thermal short-circuit effect (Serageldin et al., 2018; Zhou et al., 2021). The increase ratio of average q_{oval} and $q_{circular}$ is consistent along the operation durations in all the selected S values, except at the maximum (0.11 m), where the effect of S is increasing over time due to the minimum thermal short circuit effect between the tube legs. However, q_{oval} overlaps $q_{circular}$ tube in all the studied S values.

4.8 Tube thickness

Since the tube thickness has a relative influence on the thermal performance of GHEs (Tang and Nowamooz, 2019), two more tube thicknesses t (mm), were selected: 1.7 and 5.7, besides the standard value in this study, 3.7. To ensure a proper comparison, A for the circular and oval tubes and the shape factor (see Section 4.9) for the oval tube are kept constant during the t effect investigation. Table 5 illustrates the change ratio of the average q_{oval} and $q_{circular}$ at various tube thicknesses over the periods of operation. In general, the change ratio of average q_{oval} and $q_{circular}$ increases consistently with decreasing t; because the thinner tube wall has less thermal resistance (Tang and Nowamooz, 2019). However, a small influence was detected of the selected values of t on the two studied tube shapes within 5-6% at 24:00, and the oval tube showed a slightly greater effect of t than the circle tube.

4.9 Shape factor

For the evaluation of the effect of the geometrical parameters on the thermal performance of the oval-shaped tube GHE, the following shape factor β is introduced:

$$\beta = \frac{h}{w} \tag{1}$$

where h, and w are the height and width of the oval tube (see Figure 1). Based on eq. (1), the shape factor can be calculated, and three values of β were selected: 5, 1.8, 0.9, and besides the standard value in this paper, 3.47. To guarantee a fair comparison of the thermal performance between circular and oval tubes, the oval tube was given an identical cross-sectional area to the circular tube (Jahanbin, 2020; Zhou et al., 2021). Each shape factor of the oval tube has the same area as the standard circle tube in this paper as 835 mm^2. Table 5 displays the change ratio of average q for oval tube throughout various operational periods and β values. Figure 8 shows the average q for the shape factor effect of oval cross-section tube GHE compared to the standard circular cross-section tube GHE at 24:00. Δ increases by increasing β, as shown in Figure 8, and increasing β will guarantee a better oval tube heat transfer performance.

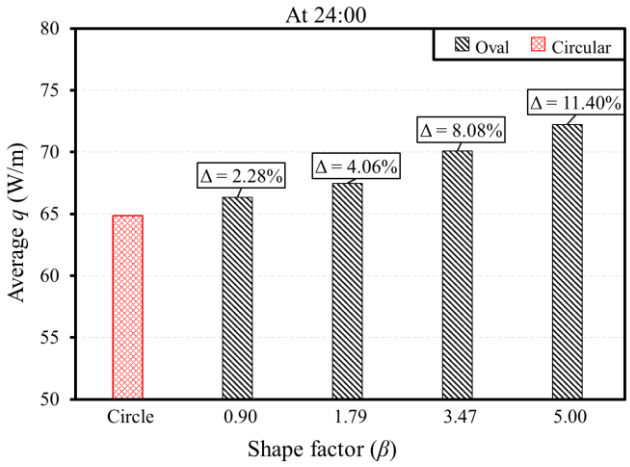

Figure 8. Average q for the shape factor effect of oval cross-section tube GHE compared to the standard circular cross-section tube GHE at 24:00.

4.10 Tube inclined angle

Figure 1 shows the tube inclined angle θ^o of the oval tube. Two more θ (^{o}) were selected in a clockwise direction: 135^o, and 180^o, besides the standard angle 90^o. The change ratio of the average q of the oval tube throughout various timeframes under the given values of θ^o is shown in Table 5. The effect of θ^o is small; only a 3% change was detected in the average q.

Table 5. The change ratio of average q of the key operating and design parameters.

Parameter	Unit	Value	Change of average q under different duration (%)					
			1:00		6:00		24:00	
			Circular	Oval	Circular	Oval	Circular	Oval
L	m	50	20.53	28.10	14.42	16.98	12.01	13.22
		90	10.07	11.11	6.56	6.98	5.29	5.54
		150	-9.28	-10.17	-6.54	-6.94	-5.50	-5.74
A		530	-13.61	-11.90	-9.14	-8.84	-6.89	-6.85
		1250	14.05	14.60	9.14	10.04	6.71	7.37
λ_{bf}	W/m·K	0.9	-7.02	-7.89	-9.68	-11.45	-8.94	-10.78
		1.2	-2.76	-3.18	-3.92	-4.68	-3.61	-4.35
		2	3.85	4.23	4.81	5.66	4.21	5.05
		2.5	6.37	7.02	7.99	9.43	6.97	8.35
λ_s	W/m·K	1.27	-3.12	-2.92	-6.52	-6.35	-8.56	-8.51
		1.34	-2.11	-1.98	-4.45	-4.34	-5.86	-5.83
		1.62	1.49	1.32	3.13	3.03	4.16	4.14
S	mm	40	-10.24	-9.71	-12.15	-11.83	-10.80	-10.32
		60	-3.89	-3.72	-5.53	-5.58	-5.03	-4.99
		110	2.96	2.54	6.03	6.21	5.75	5.90
t	mm	1.7	9.30	8.52	7.85	6.99	6.26	5.49
		5.7	-6.24	-5.97	-5.96	-5.40	-4.99	-4.43
β	-	5	-	4.41	-	3.87	-	3.07
		1.79	-	-5.21	-	-4.58	-	-3.72
		0.9	-	-7.49	-	-6.61	-	-5.37
θ	o	135°	-	-3.03	-	-2.96	-	-2.39
		180°	-	-2.59	-	-1.95	-	-1.29

5. SENSITIVITY ANALYSIS

A sensitivity analysis is implemented for the previously studied factors. Since long-term and short-term operations have various impacts on q, the sensitivity analysis includes three periods of operation: 1 hour, 6 hours, and 24 hours. Figure 9(a, b) shows the changing ratio of average q_{oval} and $q_{circular}$ over each period using a tornado diagram. The parameter with the highest sensitivity for the oval tube is M, followed by λ_{GHE}, L, and A. In addition, the effects of these parameters are prominent during the early periods of the operation. However, the influence of the parameters λ_{bf}, λ_s, S, t, β, and θ^o is limited. The sensitivity analysis indicates that the flow rate, GHE materials, GHE length, and cross-section tube area should be carefully adjusted for oval and circle tubes. Comparatively to circular tube GHE, as illustrated in Figure 9(b), previous studies (Han and Yu, 2016; Tang and Nowamooz, 2019; Kerme and Fung, 2021b) also demonstrated that M, λ_{GHE}, L, and A were the most influential parameters, which was consistent with the results of the current study.

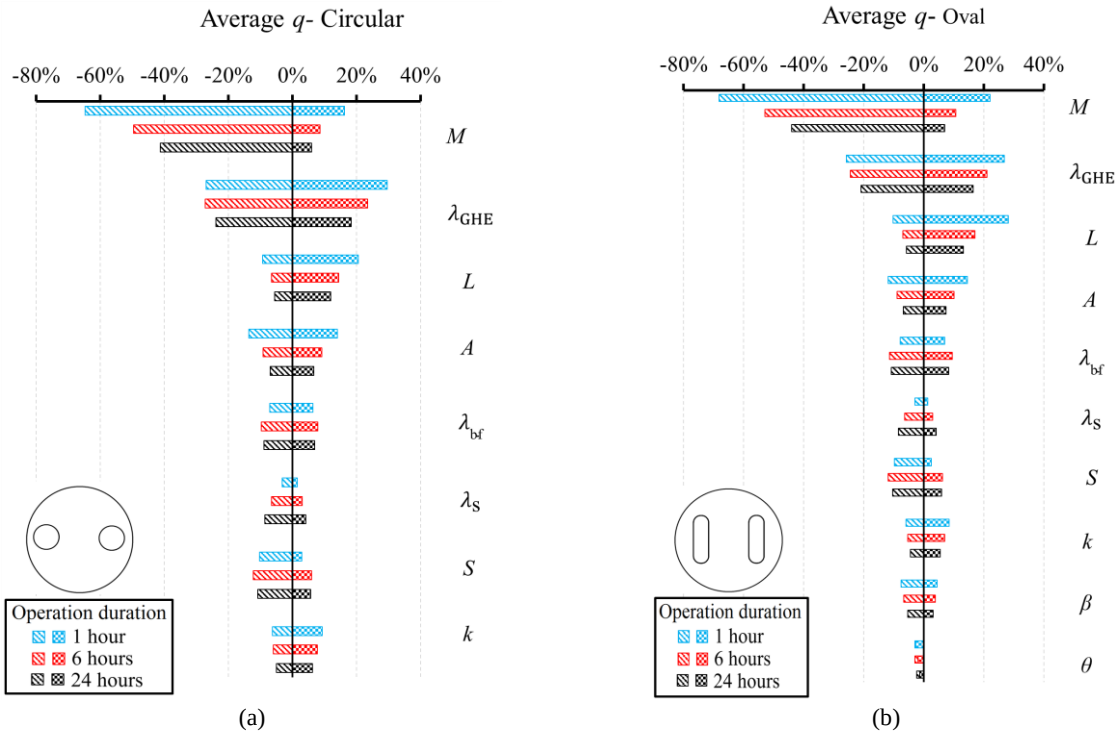

Figure 9. Sensitivity analysis for different operating durations. (a) Circle cross-section tube GHE, (b) Oval cross-section tube GHE.

Rajeh, Al-Kbodi, Li, and Zhao.

6. CONCLUSIONS

In a systematic evaluation comparison, this study used a 3-D numerical model, validated by experimental results from the literature, to compare the heat transfer performance of oval cross-section tube GHE to typical circular cross-section tube GHE. The impact of 10 significant operating and design parameters on the thermal performance of the two studied tube-shaped GHEs was compared. The following points could be concluded:

1. An excellent agreement was confirmed between the adopted numerical model and experimental data from the literature, which validates the results of the series of numerical simulations of this study.
2. Oval cross-section tube GHE outperforms the typical circular cross-section tube GHE in all the key operating and design parameters, particularly at the initial stages of the operation, in which the maximum and average heat transfer rates of oval cross-section tube GHE can be enhanced by up to 26.41% and 12.26%, respectively, compared to circular cross-section tube GHE.
3. Oval-shaped tube GHE is more promising for shallower depths than deeper ones.
4. Compared to a typical circular cross-section tube, increasing the shape factor of the oval cross-section tube will increase the heat exchange rate of the GHE.
5. The sensitivity analysis revealed that the most sensitive parameters of oval cross-section tubes are flow rate, GHE materials, GHE length, and cross-section tube area, so they should be carefully designed. However, the effects of these parameters are significant at the initial stages of the operation.

Based on the results of the present study, more insight can be gained into the oval cross-sectional shape U-tube GHE design and development for increasing the potential applications of the GSHPs and their applicable conditions.

7. REFERENCES

Aydın, M. and Sisman, A.: Experimental and computational investigation of multi U-tube boreholes, *Applied Energy*, **145**, (2015), pp. 163–171.

Dores, D. and Lautze, N.: Preliminary assessment of ground-source heat exchangers for cooling in Hawai'i, *Sustainable Energy Technologies and Assessments*, **37**, (2020), p. 100579.

Han, C. and Yu, X. B.: Sensitivity analysis of a vertical geothermal heat pump system, *Applied Energy*, **170**, (2016), pp. 148–160.

Jahanbin, A.: Thermal performance of the vertical ground heat exchanger with a novel elliptical single U-tube, *Geothermics*, **86**, (2020), p. 101804.

Jalaluddin, Miyara, A., Tsubaki, K., Inoue, S. and Yoshida, K.: Experimental study of several types of ground heat exchanger using a steel pile foundation, *Renewable Energy*, **36 (2**), (2011), pp. 764–771.

Javadi, H., Ajarostaghi, S.S.M., Pourfallah, M. and Zaboli, M.: Performance analysis of helical ground heat exchangers with different configurations, *Applied Thermal Engineering*, **154**, (2019), pp. 24–36.

Javadi, H., Ajarostaghi, S.S.M., Mousavi, S.S. and Pourfallah, M.: Thermal analysis of a triple helix ground heat exchanger using numerical simulation and multiple linear regression, *Geothermics*, **81**, (2019), pp. 53–73.

Kavanaugh, S. P. and Rafferty, K. D.: Geothermal heating and cooling: design of ground-source heat pump systems, *ASHRAE*, (2014).

Kerme, E. D. and Fung, A. S.: Heat transfer simulation, analysis and performance study of single U-tube borehole heat exchanger, *Renewable Energy*, **145**, (2020), pp. 1430–1448.

Kerme, E. D. and Fung, A. S.: Comprehensive simulation based thermal performance comparison between single and double U-tube borehole heat exchanger and sensitivity analysis, *Energy and Buildings*, **241**, (2021a), p. 110876.

Kerme, E. D. and Fung, A. S.: Comprehensive simulation based thermal performance comparison between single and double U-tube borehole heat exchanger and sensitivity analysis, *Energy and Buildings*, **241**, (2021b), p. 110876.

Li, Y., Mao, J., Geng, S., Han, X. and Zhang, H.: Evaluation of thermal short-circuiting and influence on thermal response test for borehole heat exchanger, *Geothermics*, **50**, (2014), pp. 136–147.

Li, Y., Ma, L., Xu, W., Zhu, Q., Li, W., Zhao, J. and Zhu, J.: Multi-external-chamber coaxial borehole heat exchanger: Dynamic heat transfer and energy consumption analysis, *Energy Conversion and Management*, **207**, (2020), p. 112519.

Lund, J. W. and Toth, A. N.: Direct utilization of geothermal energy 2020 worldwide review, *Geothermics*, **90**, (2021), p. 101915.

Mehrizi, A.A., Porkhial, S., Bezyan, B. and Lotfizadeh, H.: Energy pile foundation simulation for different configurations of ground source heat exchanger, *International Communications in Heat and Mass Transfer*, **70**, (2016), pp. 105–114.

Ministry of Construction in the People's Republic of China: Technical code for ground-source heat pump system (GB 50366-2009), *China Architecture and Building Press*, Beijing, (2009), [in Chinese].

Ngo, I. L. and Ngo, V. H.: A new design of ground heat exchanger with insulation plate for effectively geothermal management, *Geothermics*, **105**, (2022), p. 102512.

Noorollahi, Y., Saeidi, R., Mohammadi, M., Amiri, A. and Hosseinzadeh, M.: The effects of ground heat exchanger parameters

changes on geothermal heat pump performance – A review, *Applied Thermal Engineering*, **129**, (2018), pp. 1645–1658.

Ruan C, Feng S, M. S.: An analysis of the characteristics of thermal physical properties and their influencing factors in the Tianjin area (in Chinese)., *Hydrogeol Eng Geol*, **44 (5)**, (2017), pp. 158–63 [in Chinese].

Saeidi, R., Noorollahi, Y. and Esfahanian, V.: Numerical simulation of a novel spiral type ground heat exchanger for enhancing heat transfer performance of geothermal heat pump, *Energy Conversion and Management*, **168**, (2018), pp. 296–307.

Salmani, H. and Noee, T.: Hybrid Nanofluid Flow in a Horizontal Borehole Heat Exchanger with Twisted Tape as Turbulator, (2022).

Self, S. J., Reddy, B. V and Rosen, M. A.: Geothermal heat pump systems: Status review and comparison with other heating options, *Applied Energy*, **101**, (2013), pp. 341–348.

Serageldin, A.A., Sakata, Y., Katsura, T. and Nagano, K.: Thermo-hydraulic performance of the U-tube borehole heat exchanger with a novel oval cross-section: Numerical approach, *Energy Conversion and Management*, **177**, (2018), pp. 406–415.

Serageldin, A.A., Sakata, Y., Katsura, T. and Nagano, K.: Performance enhancement of borehole ground source heat pump using single U-tube heat exchanger with a novel oval cross-section (SUO) and a novel spacer, *Sustainable Energy Technologies and Assessments*, **42**, (2020), p. 100805.

Serageldin, A.A., Radwan, A., Sakata, Y., Katsura, T. and Nagano, K.: The Effect of Groundwater Flow on the Thermal Performance of a Novel Borehole Heat Exchanger for Ground Source Heat Pump Systems: Small Scale Experiments and Numerical Simulation, *Energies*, **13 (6)**, (2020), p.1418.

Serageldin, A.A., Radwan, A., Katsura, T., Sakata, Y., Nagasaka, S. and Nagano, K.: Parametric analysis, response surface, sensitivity analysis, and optimization of a novel spiral-double ground heat exchanger, *Energy Conversion and Management*, **240**, (2021), p. 114251.

Song, X., Shi, Y., Li, G., Yang, R., Xu, Z., Zheng, R., Wang, G. and Lyu, Z.: Heat extraction performance simulation for various configurations of a downhole heat exchanger geothermal system, *Energy*, **141**, (2017), pp. 1489–1503.

Tang, F. and Nowamooz, H.: Factors influencing the performance of shallow Borehole Heat Exchanger, *Energy Conversion and Management*, **181**, (2019), pp. 571–583.

Yang, H., Cui, P. and Fang, Z.: Vertical-borehole ground-coupled heat pumps: A review of models and systems, *Applied energy*, **87 (1)**, (2010), pp. 16–27.

Zarrella, A., Capozza, A. and De Carli, M.: Analysis of short helical and double U-tube borehole heat exchangers: A simulation-based comparison, *Applied Energy*, **112**, (2013), pp. 358–370.

Zarrella, A., De Carli, M. and Galgaro, A.: Thermal performance of two types of energy foundation pile: Helical pipe and triple U-tube, *Applied Thermal Engineering*, **61 (2)**, (2013), pp. 301–310.

Zhao, J., Li, Y. and Wang, J.: A Review on Heat Transfer Enhancement of Borehole Heat Exchanger, *Energy Procedia*, **104**, (2016), pp. 413–418.

Zhou, A., Huang, X., Wang, W., Jiang, P. and Li, X.: Thermo-Hydraulic Performance of U-Tube Borehole Heat Exchanger with Different Cross-Sections, *Sustainability*, **13 (6)**, (2021), p. 3255.